CLM-P888

A Sheath Mechanism for Negative Ion Production

F. A. Haas
A. J. T. Holmes

CULHAM
LABORATORY

AEA TECHNOLOGY

A SHEATH MECHANISM FOR NEGATIVE ION PRODUCTION

F A Haas and A J T Holmes

Culham Laboratory, Abingdon,
Oxfordshire OX14 3DB, UK.

(Euratom / UKAEA Fusion Association)

Abstract

A theoretical model is presented of electron suppression in negative ion sources using transverse magnetic fields. These fields are of short range across the plasma electrode aperture of the high voltage beam accelerator. They divert the electrons onto biassed collecting surfaces which reduce the extracted electron current by factors in excess of 100. The model describes the scaling laws of the electron supression effect and also the changes this field has on the extracted negative ion current which can be enhanced by the presence of the magnetic field.

Theory Division
Culham Laboratory

April 1990

1. Introduction

Neutral beam injection is widely used as an additional heating method in magnetically confined plasmas. Although the present fast particle energies are of order 100 keV, further work with larger and denser plasmas will require higher energies if penetration is to be achieved. The efficiency of conversion of a negative beam ion to a neutral atom is about 60% for a gas target which is much higher than positive ions and for this, and other reasons, negative ion sources for injectors have been widely investigated. However, despite much effort, the underlying physical processes involved in these sources is not fully understood. The objective of the present paper is to propose a theoretical model of some of the plasma properties associated with the negative ion production, particularly in the vicinity of the extraction aperture. As will be seen the model yields equations which are in surprisingly good agreement with experimental results obtained in the Culham negative ion source.

Negative ions are generated in a volume source which uses external magnets to produce cusp fields which confine the plasma, illustrated in fig 1 which shows the Culham source (Holmes et al (1987), McAdams et al (1988)). Some magnets are used to divide the source into two regions - a hot region where the plasma is produced and a cooler region where the negative ions are generated without significant destruction. The negative ions, once formed, are extracted and accelerated using a triode extractor which traps the electrons extracted along with the beam ions (McAdams et al (1988), Holmes & Nightingale (1986)). Recently a further magnetic field shown in Fig 2, has been applied across the orifice, which has been found to play a key role in the suppression of electrons and the enhancement of negative ion production (Bacal et al (1986), Lea et al (1989)). The results suggest that a significant fraction of the negative ions are generated in this particular region, which has a depth of about 1 cm. The magnitude of the ion current density extracted increases with increasing magnetic field, while the electron current density extracted, falls. This region, which we shall refer to as the "sheath", is the subject of the present investigation.

We begin by reviewing the physics conditions pertaining to the sheath. Temperatures are about 1 eV and are believed to be comparable for all four species of particle - neutrals (excited and unexcited), electrons, ions and negative ions; for simplicity, we shall always assume the temperatures to be the same. The neutral density is of order 8.0×10^{13} cm^{-3} and the electron and ion densities typically 10^{12} cm^{-3}. The density of excited states, N^*, is thought to be of the order of 10^{12} cm^{-3}, and the direct attachment coefficient, S_{DA}, is about 10^{-8} cm^3 s^{-1}. The electron and ion thermal velocities are the $v_{the} \simeq 5 \times 10^7$ and $v_{thi} \simeq 10^6$ cm s^{-1}, respectively. We shall assume that the dominant elastic collision processes are electron-neutral and negative ion-neutral, with the corresponding collision frequencies $\nu_e = 5 \times 10^6$ s^{-1}, $\nu^- = 10^7$ s^{-1}. The electron current density on the source side of the orifice is of order 5000 mA/cm^2, and an extracted negative ion current density of 30 mA/cm^2 is commonly obtained. The magnitude of the magnetic field at the insert (orifice) is in the range 0 to 200 gauss. Note that a potential φ is applied to the insert plate to draw an electron current across the magnetic field. Since the Debye length is small compared with the "sheath" depth, charge neutrality is well maintained. Thus $n_e + n_- = n_i$, where n_e, n_i and n_- are the electron, ion, and negative ion densities, respectively. In fact, we shall generally assume that $n_e \simeq n_i >> n_-$. To model the sheath under the above conditions we shall adopt a fluid description. We note that throughout the following work, current densities and currents are always defined in terms of the actual charges. Thus the electron current density j_e is given by $j_e = -ne\underline{v}_e$

2. Theoretical Model

Since we have no knowledge of the neutral fluid motion, we shall make the simplest assumption and set it to zero. The electron ion and negative ion fluid momentum equations take the forms

$$0 = -\nabla p_e - en_e (\underline{E} + \underline{v}_e \times \underline{B}) - n_e m_e \nu_e \underline{v}_e \quad (1)$$

$$0 = -\nabla p_i + en_i (\underline{E} + \underline{v}_i \times \underline{B}) - n_i m_i \nu_i \underline{v}_i \quad (2)$$

$$0 = -\nabla p_- - en_- (\underline{E} + \underline{v}^- \times \underline{B}) - n_- m_- \nu_- \underline{v}^-, \quad (3)$$

all symbols having their usual meanings. We shall also require the electron and negative ion continuity equations, namely,

$$\nabla . \quad (n_e \underline{v}_e) \quad = \quad - S_{DA} N^* n_e \tag{4}$$

and $$\nabla . \quad (n \underline{v}^-) = + S_{DA} N^* n_e, \tag{5}$$

where the right-hand sides represent the electron attachment process.

The actual geometry of the "sheath" region is complicated and so we consider the representative model situation shown in fig. 2. This takes the form of a rectangular slit of height, depth and length, 2b, a and L, respectively. We assume rectangular coordination x, y, z based on the point 0, the x-direction being into the plane of the paper. A constant uniform magnetic field, B, is taken in the x-direction. We further assume that all gradients with respect to x are zero so that our formulation is two-dimensional.

2.1 Electron Flow

We begin our analysis by considering the ion momentum equation. Since experiment suggests that any ion currents present are very small, we shall make the assumption that the ion fluid velocity is zero. Thus the electric field is determined from the equation

$$e \, n_i \, \underline{E} \quad = \quad \nabla p_i \tag{6}$$

Making the further assumption that $E_y = 0$, then it immediately follows that $p_i = p_i(z)$, and hence

$$E_z = \frac{1}{e n_i} \frac{dp_i}{dz} \tag{7}$$

We now turn to the electron momentum equation. Since $n_e \simeq n_i$, we must have $\frac{dp_e}{dy} \simeq \frac{dp_i}{dy} = 0$, and therefore the y-component gives

$$v_{ez} \quad = \quad - \frac{m_e \nu_e}{eB} v_{ey} \tag{8}$$

Taking the z-component, the first three terms of equation (1) yield (on setting $n_e \simeq n_i$),

$$n_e \, v_{ey} \simeq \frac{2}{eB} \, \frac{dp_e}{dz} \tag{9}$$

In equation (9) collisions have been neglected, as the use of equation (8) shows this term to be of order $(\frac{\nu_e}{\omega_e})^2$ down on those retained, ω_e being the electron cyclotron frequency, $\omega_e = \frac{eB}{m_e}$; for B = 10 g the quantity

$(\frac{\nu_e}{\omega})^2 \simeq 10^{-3}$.

We note that p_e is a function of z only. If we further assume that T = T(y) only, then $p_e = n_e \, T$ leads to

$$p_e(z) = n_e(y,z) \; T(y), \tag{10}$$

implying the cancellation of the y-dependence. Note T(y) and other temperature is defined in units of joules.

We next consider the electron continuity equation. Assuming the sink (electron attachment to excited neutrals) to be unimportant, and using equation (8), then the relevant form for electron continuity is

$$\frac{\partial}{\partial y} (n_e \, v_{ey}) - \frac{\nu_e}{\omega_e} \, \frac{\partial}{\partial z} (n_e \, v_{ey}) = 0 \tag{11}$$

A solution of equation (11) is given by

$$n_e \, v_{ey} = - A \exp(- \gamma z) \exp\left(- \frac{\nu_e}{\omega_e} \, \gamma \, y \right) \tag{12}$$

where A and γ are constants. Now we anticipate that the z-variation in equation (12) is "rapid", while the y-variation is "slow". Thus we set the y exponential to unity - this will be checked a posteriori. Substituting equation (12) into equation (9) and integrating, we obtain

$$n_e \, (y, \, z) = n_e \, (y, \, 0) \exp(- \gamma z) \tag{13}$$

where

$$n_e\ (y,0) \;=\; \frac{1}{T(y)} \cdot \frac{A\ e\ B}{\gamma}$$

To determine γ we observe that the electron fluid velocity at the insert surface ($y = -b$) is given in terms of the applied "sheath" potential, that is

$$v_{ey}\ (-b) \;=\; -\frac{v_{the}}{4}\ \exp(-\eta) \tag{14}$$

where $\eta = e\varphi/T(-b)$. Using equations (9) and (13) again, we obtain

$$\gamma \;=\; \frac{v_{the}}{8}\ \exp(-\eta)\ \frac{e\ B}{T(\ b)} \tag{15}$$

We now check the assumption that the y-variation on the right of equation (12) is unimportant. Using equation (15) and substituting typical frequencies and temperatures, and setting $\eta = 0.5$ we find that this exponential factor has fallen to only 0.99 for $y = 1.0$ cm.

We now consider the integrated version of the electron continuity equation. Assuming the electron current drawn into the extraction region is small, and electron attachment is negligible, then the total electron current entering the sheath and that drawn to the lower face of the insert will be approximately the same. Thus we derive

$$\int_{-b}^{b} j_{ez}\ (y,\ 0)\ dy \;=\; -\int_{0}^{a} j_{ey}\ (-b,\ z)\ dz \tag{16}$$

Now if j_{ep} is the average saturation current drawn in the z-direction (on the source side), we can write

$$L\int_{-b}^{b} j_{ez}\ (y,\ 0)\ dy \;=\; 2b\ L\ j_{ep}\ \exp(-\eta) \tag{17}$$

The insert current, I_{insert}, is given by

$$I_{insert} = - L \int_0^a j_{ey} (- b, z) \, dz$$

$$= e L \int_0^a n_e (- b, z) \, v_{ey} (- b) \, dz$$

Using equations (13), (14) and (15), it is straightforward to derive

$$I_{insert} = - \frac{2 T(- b)}{B} L \, n_e (- b, 0) \tag{18}$$

where we have neglected $\exp(- \gamma a)$ compared to unity. From equations (17) and (18) we obtain

$$n_e (- b, 0) = - \frac{bB}{T(- b)} \, j_{ep} \exp(- \eta) \tag{19}$$

where we note that j_{ep} is negative.

We now evaluate the electron current density leaving the orifice and entering the extraction region. This is given by

$$j_{ez} = - e \, n_e \, v_{ez} = \frac{m_e \, n_e \, \nu_e \, v_{ey}}{B} \tag{20}$$

Now by equations (9), (13) and (15),

$$v_{ey} = - \frac{1}{4} \frac{T(y)}{T(- b)} \, v_{the} \exp(- \eta) \tag{21}$$

and substituting into equation (20), yields

$$j_{ez}(a) = \frac{\nu_e}{2} \frac{\exp(- 2\eta)}{v_{the}} b \, j_{ep} \exp\left[- \frac{v_{the}}{8} \exp(- \eta) \frac{e B a}{T(- b)} \right] \tag{22}$$

To obtain this result we have set $n_e(y, 0)\ T(y) = n_e(-b, 0)\ T(-b)$, used $m_e\ v_{the}^2 = 2T(-b)$, and substituted for $n_e(-b, 0)$ from equation (19). The above expression for $j_{ez}(a)$ can be directly compared with experiment. Figure 3 shows the variation of $j_{ez}(a)$ with B for fixed j_{ep}, T, a and b. The exponential law is found to hold over a range of 10^2 and the slope yields a value of T which is close to that measured by other diagnostics. A further way in which this theory can be compared with experiment can be made by a simple rearrangement of equation (22). Thus we write

$$\ell n \left(\frac{j_e(a)}{I_{insert}} \right) = -\eta + \ell n \left(\frac{\nu_e}{4\ v_{the}\ L} \right) - \frac{e\ B\ v_{the}\ I_{insert}\ a}{16\ T(-b)\ b\ L\ j_{ep}} \qquad (23)$$

where we have used equation (18). A plot of $\ell n \left(\frac{j_{ze}(a)}{I_{insert}} \right)$ against I_{insert} is shown in fig. 4. The graph shows a straight line dependence, the slope increasing with B. For large η, the first term on the right-hand side of equation (23) becomes important, and this can be seen in the results when I insert becomes small (ie η is about 3 for hydrogen).

2.2 Negative Ion Flow

We now investigate the negative ion current. Neglecting the pressure gradient and $\underline{v}^- \times \underline{B}$ terms in the z-component of the negative ion momentum balance, equation (3), we have

$$v_z^- = -\frac{e\ E_z}{m_-\ \nu_-} \qquad (24)$$

The approximations made will be checked a posteriori. Noting that $n_i \simeq n_e$, and using equations (7), (13) and (15), v_z^- can be written as

$$v_z^-(y) = \frac{v_{the}}{8\ m_-\ \nu_-} \exp(-\eta)\ e\ B\ \frac{T(y)}{T(-b)} \qquad (25)$$

The continuity equation for the negative ion current density is

$$\frac{\partial j_z^-}{\partial z} = - e N^* S_{DA} n_e - \frac{\partial j_y^-}{\partial y} \qquad (26)$$

If we treat the second term on the right-hand side as small, then we can straightforwardly integrate equation (26) and obtain the negative ion density. Thus:

$$n^-(y, z) = n^-(y,0) + \frac{N^* S_{DA}}{v_z^-(y)} \int_0^z n_e(y, z)\, dz \qquad (27)$$

where $v_z^-(y)$ is known from equation (25). Substituting for $n_e(y, z)$ this becomes

$$n^-(y, z) = n^-(y, 0) + \frac{N^* S_{DA}}{\gamma\, v_z^-(y)} n_e(y, 0) \left[1 - \exp(-\gamma z) \right] \qquad (28)$$

Returning to the full continuity equation, equation (26), and defining the y-average

$$< F(z) > \equiv \frac{1}{2b} \int_{-b}^{b} F(y, z)\, dy \qquad (29)$$

we derive

$$< j_z^-(a) > = < j_z^-(0) > - \frac{e N^*}{2b} S_{DA} \int_{-b}^{b} \int_0^a n_e(y, z)\, dy\, dz$$

$$- \frac{e}{2b} \int_0^a n_-(-b, z)\, v_y^-(-b)\, dz \qquad (30)$$

where we have assumed that a negative ion flux is drawn to the lower insert surface at y = -b by the applied bias field; it is further assumed, for simplicity, that there is no negative ion flux at the surface at y = b.

Thus, as with the electrons, we set

$$v^-_y(-b) = -\frac{v^-_{th}}{4} \exp(-\eta) \tag{31}$$

Substituting from equations (13) and (28), the integrations in equation (30) can now be carried through, and we derive

$$\langle j^-_z(a) \rangle = \langle j^-_z(0) \rangle + \frac{e N^* S_{DA}}{\gamma} \langle n_e(0) \rangle [\exp(-\gamma a) - 1]$$

$$+ \frac{e}{8b} v^-_{th} \exp(-\eta) \left\{ a\, n^-(-b, 0) + \frac{N^* S_{DA}\, n_e(-b, 0)}{\gamma\, v^-_z(-b)} [a + \frac{1}{\gamma} (\exp(-\gamma a) - 1)] \right\} \tag{32}$$

From the electron physics

$$n_e(y, z)\, T(y) = n_e(-b, z)\, T(-b) \tag{33}$$

so that

$$\langle n_e(0) \rangle = n_e(-b, 0)\, T(-b) \left\langle \frac{1}{T} \right\rangle \tag{34}$$

Now provided the temperature at the insert surfaces ($y = \pm b$) is of a similar magnitude but less than the central temperature $T(0, 0)$, then it is sufficiently accurate to set $T(-b) \left\langle \frac{1}{T} \right\rangle \simeq 1.0$. This can be simply demonstrated for a parabolic temperature profile. It follows that

$$\langle n_e(0) \rangle \simeq n_e(-b, 0) = \frac{-bB}{T(-b)} j_{ep} \exp(-\eta) \tag{35}$$

Neglecting exponential factors as small compared to unity, substituting for γ and $v_z^-(-b)$ from equations (15) and (25), and using equation (35), we express equation (32) in the form

$$j_z^-(a) > = < j_z^-(0) > + \frac{ea}{8b} v_{th}^- \exp(-\eta)\ n^-(-b, 0)$$

$$+ \frac{8\ N^*\ S_{DA}\ b\ j_{ep}}{v_{the}} \left\{ 1 - \frac{B_{C1}}{B} + \frac{B_{C1}\ B_{C2}}{B^2} \right\} \quad (36)$$

The characteristic magnetic fields, B_{c1} and B_{c2}, are defined to be

$$B_{c1} = \frac{a}{b} \frac{v_{th}^-}{v_{the}} \frac{m^- v^-}{e} \quad \text{and} \quad B_{c2} = \frac{4\ m_e\ v_{the}}{a\ e} \exp(+\eta) \quad (37)$$

Figure 5 shows a comparison of the average negative ion current calculated from equation (36) with that measured in the Culham experiment.

It is now necessary to check on the several approximations which have been made in deriving equation (36). It is clear that for sufficiently large B the exponential factors neglected in the above are totally unimportant. For B = 30 g and parameters typical of the experiment, $\exp(-\gamma a) \simeq 0.2$, so that no serious error is incurred. In deriving equation (36) an iterative approach was followed, and this implies that the second term on the right-hand side, as well as the terms involving B, should be small. Clearly, for sufficiently large B, that is, greater than B = 30 g, the latter terms will always be small. Taking a = 1 cm and b = 4 cms and assuming $\eta = 0.5$ then the second term on the right-hand side of equation (36) is small compared with

$$\frac{8\ N^*\ S_{DA}\ b\ j_{ep}}{v_{the}}$$

provided $n^-(-b, 0)/n_e(0,0) \leq 0.1$. Finally we must check the neglect of the $\underline{v}^- \times \underline{B}$ and negative ion pressure gradient terms in deriving equation (24). Now from equation (25) we estimate the magnitude v_z^- to be of order 2×10^5 cms^{-1} for B = 20 g. In the y-component of equation (3) we set $\frac{\partial p^-}{\partial z}$

to balance the collision term, and this gives $v_y^- \sim 10^5$ cm s^{-1}; using the above value for v_z^-, the v_z^- B term is about 10^{-2} of the $\frac{\partial p^-}{\partial z}$ term, and can be rightfully neglected. Turning to the z-component, using the above estimates for v_y^- and v_z^-, it is straightforward to show that the v_y^- B term is also 10^{-2} of the collision term, and can be neglected.

Substitution of equation (28) into the $\frac{\partial p^-}{\partial z}$ term and comparison with the collision term in the z-component of the momentum balance equation, allows us to check on the neglect of the former term.

For B = 20 g it is found that this is justified if $n^-/n_e(-b,o) \gtrsim 3\%$. However, this restriction is eased with increasing B, and at B = 100 g, the condition $n^-/n_e \gtrsim 1\%$ is adequate.

3. Discussion and Conclusions

The scaling of $< j_z^- (a)$ with B has been checked by experiment using the facility as that which derived the results in figures 3 and 4. In figure 5 the extracted negative ion current density j^- (corrected for any stripping losses) is plotted as a function of B^{-1}. The experimental results yield an impirical expression of:

$$J_- = \alpha - \beta/B$$

$$\simeq <j^-_z (a)>$$

This has been compared with the equation (36) which defines:

$$\alpha = < j_z^- (o) > + \frac{ea}{8b} v_{th}^- \exp(-\eta) . n^- (-b,o) + \frac{8N^* S_{DA} b j_{ep}}{v_{the}}$$

$$\beta = 8N^* S_{DA} b j_{ep} . \frac{a}{b} \frac{v_{th}^- m^- \nu^-}{v_{the}^2 e} \qquad (38)$$

No evidence of a B^{-2} scaling term is seen but this would be difficult to extract from the existing data. The value of $\langle j^-_z\ (o)\rangle$ and the product $en^-\ (-b,o).v^-_{th}$ are both essentially the negative ion flux which is produced in the main volume of the discharge, well away from the region considered in this paper. We can replace these two terms by using a simple particle balance in the main plasma (Holmes et al 1987) where:

$$N_+\ N_-\ S_{ii} = N_e\ N^*\ S_{DA}$$

where S_{ii} is the ion-ion recombination rate which is the main plasma volume loss process and N_+, N_- and N_e are the plasma densities well away from the aperture.
Hence for $N_+ \simeq N_e$:

$$\langle j^-_z\ (o)\ \rangle \simeq en^-(-b,o)v^-_{th} = \frac{N_e}{N_+}\frac{S_{DA}}{S_{ii}}\ N^*\ ev^-_{th} \simeq \frac{S_{DA}}{S_{ii}}\ Ne^*\ v^-_{th}$$

$$\text{Thus } \alpha \simeq \langle j^-_z(0)\rangle .\ \left(1 + \frac{a\ e^{-\eta}}{8b}\right) + \langle j^-_z(0)\rangle .\ \frac{8b\ j_{ep}\ S_{ii}}{e\ v^-_{th}\ v_{the}} \qquad (39)$$

$$\beta \simeq \langle j^-_z(0)\rangle .\ \frac{8\ j_{ep}\ a\ m^-v^-S_{ii}}{e^2\ v^2_{th}} = \frac{8N^*S_{DA}j_{ep}a\ m^-v^-_{th}}{e\ v^2_{the}} \qquad (40)$$

It is useful to compare the slope in fig.5 with the theoretical value of β given above. Bruneteau and Bacal (1985) give values for the negative ion-neutral atom collision frequency of 4.10^{-15} N [sec^{-1}] where N is the gas density and also a value for the ion-ion recombination rate, S_{ii}, of about 3.10^{-13} [$m^3\ s^{-1}$]. The values of j_{ep} and a for this set of data in a hydrogen discharge were 1.4 10^4 [A/m^2] and 0.015 [m] respectively and N was 4.2 10^{20} [m^{-3}] (ie 12mT). Hence the theoretical value of β for T_e equal to 0.5 eV is:

$$\beta = 0.04\ [TA\ m^{-2}]$$

which should be compared with an experimental value for β of 0.075 [TA m^{-2}]. Assuming that T_- equals T_e then we find that N^*S_{DA} is

$$N^* S_{DA} \simeq 1.1\ 10^5$$

$$\text{or} \quad \frac{N^*}{N} \simeq 0.026$$

This value is not inconsistant with calculations by Hiskes et al (1985).

The importance of the product $N^* S_{DA}$ can be examined by comparing the H_2 and D_2 discharge results shown in fig 5. For low magnetic fields the ratio of the currents is about 1.4 which is largely determined by the first term in the expression for α above. This ratio almost certainty results from an isotope effect in the cross-sections plus the lower drift velocity arising from the heavier D^- ion. This has been reported by Holmes et al (1987). However, the slopes are virtually identical as the product of $\bar{m}\,\bar{v}_{th}$ will be probably larger by a factor of about $\sqrt{2}$ for deuterium.

The model breaks down for very small fields as the electrons become demagnetised but this should give a value of j_- of

$$j_- = \frac{S_{DA}\ N^*\ e\ v_{the}}{S_{ii}}$$

which is the first term in the expressions for α in equation 39.

The above work indicates that under the right conditions, the magnetic field which is used to suppress the electrons can enhance the negative ion yield. However it should be noted that the presence of the field structure used to create the field may cause loss of plasma and result in a lower negative ion yield that would be the case if this structure was omitted entirely. However the above results taken together with the electron results described in figures 3 and 4 provide a description of the effects of electron suppression which is vital element in the long term objective of neutral beam sources at high energy.

Acknowledgements.

The authors would like to thank JET for financial support through an Article 14 contract and in particular Drs R Hemsworth and E Thompson. Also we would like to thank Dr L. Lea and Mr M. Thornton who carried out much of the experimental work mentioned above.

References

1 A J T Holmes, L M Lea, A F Newman and M P S Nightingale, Rev. Sci. Instrum., 58, pp223-234, (1987)

2 R McAdams, A J T Holmes and M P S Nightingale, Rev. Sci. Instrum, 59, pp895-901, (1988)

3 A J T Holmes and M P S Nightingale, Rev. Sci. Instrum. 57, pp2402-2408, (1986)

4 M Bacal, J Bruneteau, P Devynk and F Hillion, Proc 4th Symp. Production and Neutralisation of Neg. Ions and Beams, Brookhaven Nat. Lab., Upton, N.Y., USA, (1986)

5 L M Lea, T M Thornton and A J T Holmes, Proc. Ion Source Conf. Lawrence Berkeley Lab., Berkeley, USA, (1989)

6 J M Wadehara, Appl Phys Lett. 35, pp917-919, (1979)

7 J Bruneteau and M Bacal, J. Appl. Phys., 57, pp4342-4348, (1985)

8 J Hiskes, A M Karo and P A Willman, J. Vac. Sci. Tech., A3(3), pp1229-1233, (1985)

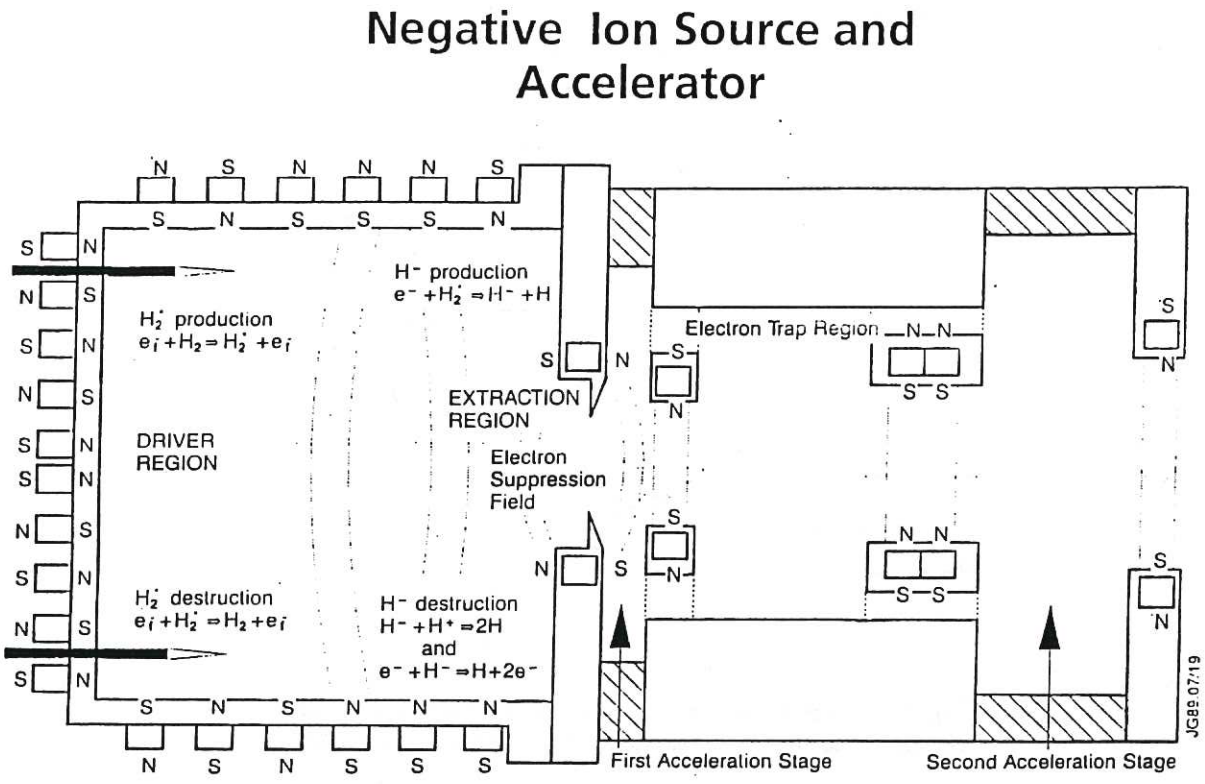

Fig. 1 A illustration of a negative ion source showing the plasma source fields and the extraction aperture

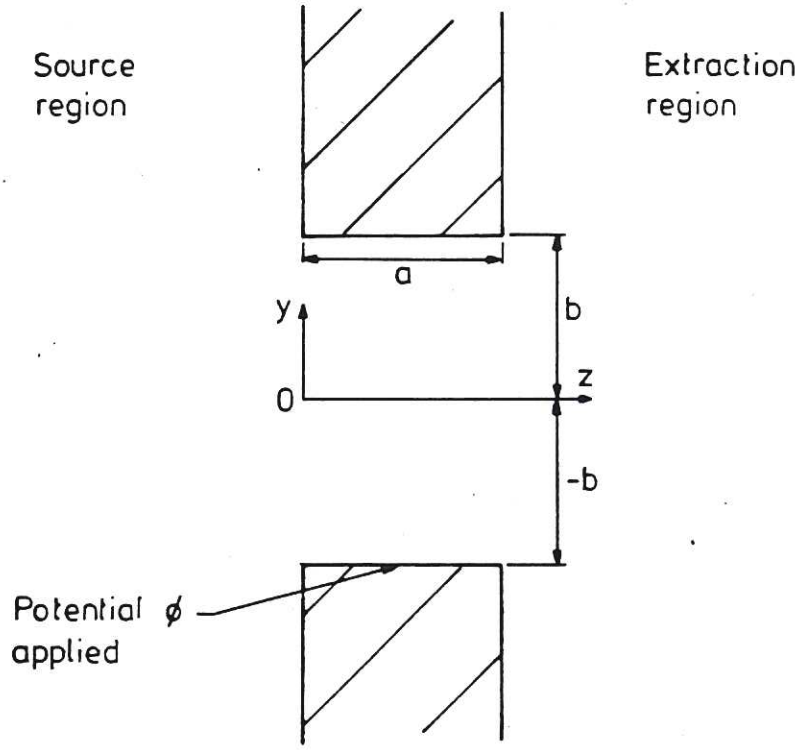

Fig. 2 An illustration for the extraction aperture. The shaded area is the electrode and the magnetic field is into the plane of the diagram.

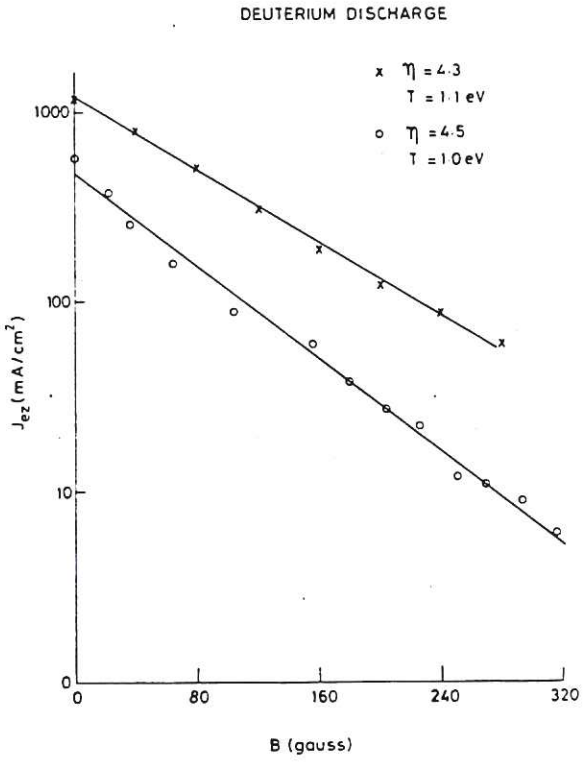

Fig. 3 Experimental variation of the extracted electron current density with magnetic field. An exponential dependence is seen according to equation 22.

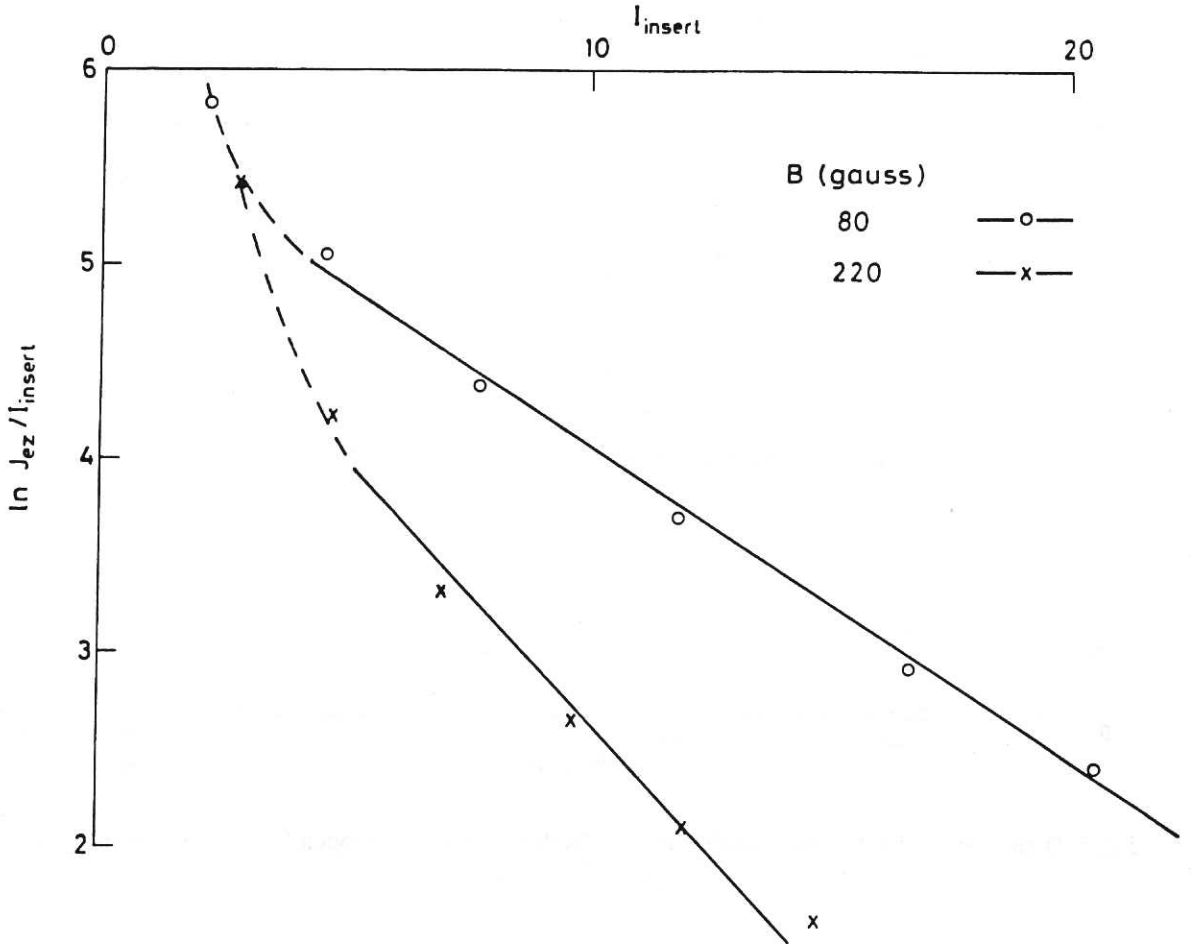

Fig. 4 The logarithm of j_e/I_{insert} is plotted against I_{insert} for two values of B. When I_{insert} is small, the value of η large and the straight line dependence breaks down as indicated by equation 23 and the dashed lines.

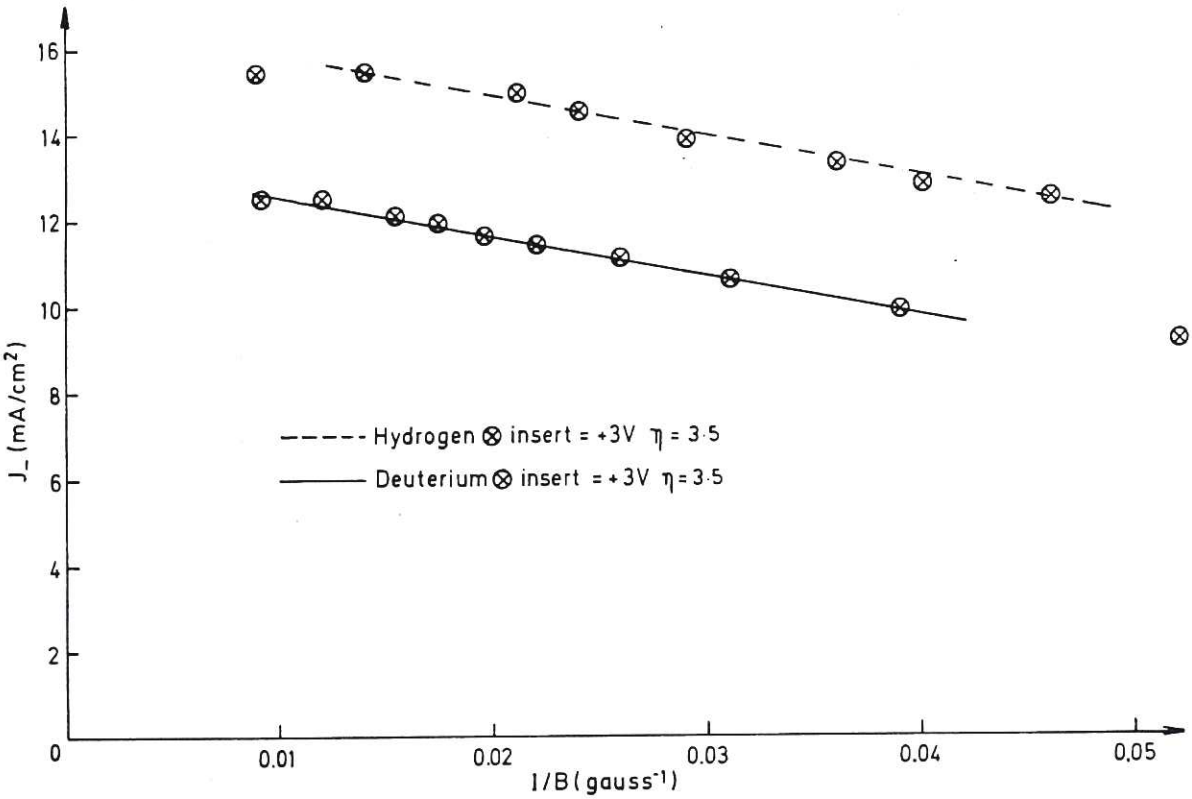

Fig. 5 Dependence of extracted negative ion flux in deuterium or hydrogen for an arc current of 400 A at 12 mT pressure.